Mesozoic 003 (2): 165–176
https://www.mapress.com/mz/

Article

ISSN 3021-1859 (print edition)
MESOZOIC
ISSN 3021-1867 (online edition)

https://doi.org/10.11646/mesozoic.3.2.3
http://zoobank.org/urn:lsid:zoobank.org:pub:0EE54F4D-2116-4680-84E5-42984DA11615

Early Cretaceous amber from the Heibaoshan-Handaqi Basin, Heilongjiang Province, Northeast China

LING-HAN LUO[1, 2], XIAO-KAI YANG[1, 2], CHONG DONG[1], XIN SUI[1, 2], DANY AZAR[1, 2, 3], JIAN GAO[1] & DI-YING HUANG[1, 2, *]
[1]*State Key Laboratory of Palaeobiology and Stratigraphy, Nanjing Institute of Geology and Palaeontology, Chinese Academy of Sciences, Nanjing 210008, China*
[2]*University of Chinese Academy of Sciences, Beijing 100049, China*
[3]*Faculty of Sciences II, Natural Sciences Department, Lebanese University, Fanar-El-Matn, PO Box 90656 Jdeideh, Lebanon*
lhluo@nigpas.ac.cn; https://orcid.org/0009-0001-6941-7547
yxk1169738053@outlook.com; https://orcid.org/0009-0000-8886-4310
cdong@nigpas.ac.cn; https://orcid.org/0000-0001-9983-4352
xinsui@nigpas.ac.cn; https://orcid.org/0009-0001-6012-4684
danyazar@ul.edu.lb; https://orcid.org/0000-0002-4485-197X
Jiangao@nigpas.ac.cn; https://orcid.org/0000-0001-8817-8599
dyhuang@nigpas.ac.cn; https://orcid.org/0000-0002-5637-4867
**Corresponding author*

Abstract

Cretaceous amber plays a crucial role in understanding the evolution of Late Mesozoic biotas and changes in palaeoclimates and palaeoenvironments. This paper reports amber, insects and plant fossils from the Lower Cretaceous Jiufengshan Formation in Heihe City, Heilongjiang Province, Northeast China, and presents the Fourier-transform infrared (FT-IR) spectroscopic characteristics of the amber. The Heihe amber occurs predominantly as irregular blocky pieces and layered forms, and is mainly preserved in coal seams. In addition, insect fossils belonging to multiple groups, including Coleoptera, Orthoptera, Hemiptera, Blattodea and Trichoptera (caddis cases), have been found in black shales near the amber-bearing horizons, further enriching the palaeobiological assemblage of the region. This discovery provides important empirical evidence for investigating the biotic characteristics and stratigraphic correlation of northern China during the late Mesozoic.

Keywords: Jiufengshan Formation, Heihe amber, FT-IR analysis, Lower Cretaceous

Introduction

The Cretaceous represents a key interval in Earth's evolutionary history, characterized by typical greenhouse climate conditions and accompanied by rapid biotic turnover and extensive diversification of organismal groups (Huber *et al*., 2002; Delclòs *et al*., 2023). Cretaceous amber-bearing deposits are mainly distributed in the Northern Hemisphere. Based on the shared characteristics of Cretaceous amber, researchers have formally established the Cretaceous Resinous Interval (CREI) to denote a period of massive resin production in Earth history (Delclòs *et al*., 2023). This interval was driven by a greenhouse climate with elevated temperatures, high atmospheric CO_2 levels, and widespread wildfires, which promoted the proliferation of resin-producing conifers and enhanced resin secretion and preservation (Delclòs *et al*., 2023).

Cretaceous amber deposits are widely distributed globally; among them, Burmese amber is the most renowned and preserves abundant bioinclusions (*e.g*., Grimaldi *et al*., 2002; Ross, 2024); additionally, Cretaceous amber outcrops have also been documented in Lebanon (*e.g*., Maksoud *et al*., 2022), Spain (*e.g*., Delclòs *et al*., 2007; Najarro *et al*., 2010), France (*e.g*., Néraudeau *et al*., 2008), the United States (*e.g*., Langenheim *et al*., 1960; Grimaldi *et al*., 1989), the Taimyr region of Russia (*e.g*., Perkovsky & Vasilenko, 2019), the Congo (*e.g*., Bouju & Perrichot, 2020), western Canada (*e.g*., McKellar *et al*., 2008), the United Kingdom (*e.g*., Tihelka *et al*., 2023), northern Japan (*e.g*., Kubota *et al*., 2025) and Antarctica (*e.g*., Klages *et al*., 2024).

Cretaceous amber occurrences in China remain relatively rare. The confirmed Cretaceous amber localities mainly include Hulun Buir amber from the late Aptian Damoguaihe Formation and the overlying

Submitted: 1 Jun. 2026; accepted by Z. Feng: 11 Jun. 2026; published: 24 Jun. 2026

Aptian–Albian Yimin Formation of the Early Cretaceous in Inner Mongolia; amber from the Early Cretaceous Dongning Formation in SE Heilongjiang Province; the Late Cretaceous Taipinglinchang Formation in North Heilongjiang Province; Late Cretaceous Xixia amber in Henan Province; as well as Late Cretaceous amber from the Dalangshan and Yetang formations in Guangdong Province (Shi *et al*., 2014; Azar *et al*., 2019; Ni *et al*., 2023; Li *et al*., 2023b; Gao *et al*., 2024; Song *et al*., 2024; Bugdaeva *et al*., 2025; Ji *et al*., 2025; Luo *et al*., 2026). Despite these discoveries, the Cretaceous amber record in China remains sparse, which limits our understanding of the evolution of regional terrestrial ecosystems and resin-producing floras.

Here we report the discovery of an Early Cretaceous amber outcrop, along with associated insects and plants, from the Heibaoshan-Handaqi Basin in North Heilongjiang Province, northeastern China. This amber occurrence falls within the CREI.

Geological setting

The Heibaoshan-Handaqi Basin, also referred to as the Heibaoshan-Mu'erqi Basin, is situated in northern Heilongjiang Province at the junction between the Great Xing'an Range and the Lesser Xing'an Range. It is superimposed on the Paleozoic Duobaoshan Island Arc Belt between the Xing'an Block and the Songnen Block (Yang *et al*., 2020). It is one of the major coal-accumulating basins in Heilongjiang Province (Zhao *et al*., 1991). The stratigraphic succession of the Heibaoshan-Handaqi Basin comprises, from bottom to top, the Early Cretaceous Guanghua Formation, Jiufengshan Formation, Ganhe Formation, and the Miocene Sunwu Formation (Yang *et al*., 2020).

The Jiufengshan Formation is the dominant coal-bearing unit in the region. Apart from the Heibaoshan-Handaqi Basin, it is widely distributed in the northern part of the Great Xing'an Range and the northwestern slope of the Lesser Xing'an Range, occurring mainly in the Dayangshu Basin, Huma Yiziquan, Fanshentun and other localities (Yang *et al*., 2020). The formation shows little lithological variation across the region, and generally represents a succession of continental volcanic-sedimentary coal-bearing strata, dominated by light gray sandstone, pebbly sandstone, tuffaceous sandstone and grayish-black mudstone, with interbeds of pyroclastic rocks and basalt (Bureau of Geology and Mineral Resources of Heilongjiang Province, 1997).

The Jiufengshan Formation yields abundant fossils, including fishes, insects, bivalves, plant macrofossils and sporopollen grains (Heilongjiang Provincial Bureau of Geology and Mineral Resources, 1993; Jin, 1997; Han *et al*., 2000). The Jiufengshan Formation in the Naketa area of Inner Mongolia has been suggested to preserve the E-E-L (*Eosestheria*-*Ephemeropsis*-*Lycoptera*) assemblage of the Jehol biota, which is considered an important record of the northern distribution of the Jehol biota (Li & Reisz, 2020; Li *et al*., 2023a). Guo (2024, unpublished master's to thesis) discovered amber in coal seams of the Jiufengshan Formation at the Gulianhe Coal Mine in the Hola Basin, but did not conduct detailed research on these materials. In the adjacent Hola Basin, the Jiufengshan Formation comprises a lower sandy conglomerate member, a middle sand-mudstone member, and an upper coal-bearing member with a persistent tuff marker bed, unlike the tuffaceous sandstone-mudstone succession with pyroclastic interbeds and basalt in the Heibaoshan-Handaqi Basin. Palynofloras in the Hola Basin are dominated by fern spores, whereas both sporopollen and plant macrofossils in the Heibaoshan-Handaqi Basin are overwhelmingly gymnosperm-dominated and yield no angiosperms (Yang *et al*., 2020).

The Jiufengshan Formation in the Heibaoshan-Handaqi Basin has not yielded the E-E-L assemblage of the Jehol biota, but contains abundant plants and sporopollen grains. Macrofossil plants are overwhelmingly dominated by gymnosperms, with no angiosperms recovered; among the plants, conifers include: *Pityostrobus sp*., *P*. cf. *dunkeri*, *Pityocladus* sp., *P*. cf. *zhalainoerensis*, *Pityophyllum* sp., *Podozamites* sp., *Elatocladus* cf. *manchuricus*, *Elatides* sp., *Pagiophyllum* sp.; cycads include: *Pterophyllum* sp., *Zamites* sp.; ginkgophytes include: *Ginkgoites* sp., *Sphenobaiera* sp.; czekanowskiales include: *Phoenicopsis* sp., *Czekanowskia rigida*; ferns include: *Coniopteris* sp., *C. burejensis*, *Cladophlebis* cf. *acuta*, etc. (Yang *et al*., 2020).

The sporopollen assemblage of the Jiufengshan Formation in the Heibaoshan-Handaqi Basin is assigned to the *Piceaepollenites*-*Appendicisporites*-*Cicatricosisporites* assemblage, which is dominated by gymnosperm pollen, with no angiosperm pollen identified (Yang *et al*., 2020). Gymnosperm pollen includes: *Piceaepollenites* sp., *P. exilioides*, *Pinuspollenites* sp., *P. divulgatus*, *Cycadopites* sp., *Classopollis annulatus*, *Abietineaepollenites*, *Cedripites*, *Parrisaccites*, *Parcisporites*, *Psophosphaera*, *Araucariacites*, *Podocarpidites* sp., *Ginkgo*, *Laricoidites*, *Inaperturopollenites*; pteridophyte spores include: *Cicatricosisporites* sp., *C. australiensis*, *C. minutaestriatus*, *C. minor*, *Fixisporites tortus*, *Aequitriradites spinulosus*, *Concavissimisporites* sp., *C. punctatus*, *C. variverrucatus*, *Deltoidospora* sp., *Gleicheniidites delicatus*, *G. senonicus*, *Gleicheniidites* sp., etc. (Yang *et al*., 2020). The assemblage is dominated by conifer pollen (*Piceaepollenites* and *Pinuspollenites*), with minor fern spores and a low abundance of

Classopollis, indicating a coniferous forest and a subtropical humid climate favorable for coal formation (Yang *et al*., 2020). In addition, early angiosperm pollen was discovered for the first time in the upper member of the Jiufengshan Formation in the Dayangshu Basin, eastern Great Xing'an Range, recording the early expansion of angiosperms in mid-latitude regions (Zhang *et al*., 2026).

Zircon U-Pb dating of the Jiufengshan Formation in different basins indicates that its deposition spanned a potentially long interval, from the Barremian to the latest Aptian. The Lower Member of the Jiufengshan Formation in the Naketa area, Inner Mongolia, was deposited from the Barremian to the earliest Aptian, yielding ages of 121.6 ± 0.47 Ma (Li & Reisz, 2020) and 124.3 ± 1.5 Ma, 124.9 ± 1.6 Ma, 121.5 ± 1.4 Ma (Li *et al*., 2023a). A tuff from the Upper Member of the Jiufengshan Formation in the Dayangshu Basin yields an age of 115.3 ± 1.4 Ma (Zhang *et al*., 2026). The maximum depositional age of the Jiufengshan Formation in the Nenjiang area, constrained by detrital zircons, is 116 ± 1 Ma (Jia *et al*., 2025). The lower tuff of the Jiufengshan Formation in the Heibaoshan-Handaqi Basin yields a crystallization age of 119 ± 0.89 Ma (Yang *et al*., 2020). Collectively, these data demonstrate that the Jiufengshan Formation spans the entire interval from the Barremian to the latest Aptian. Our sampling locality is adjacent to that of Yang *et al*. (2020), and the strata correspond to their second member of the Jiufengshan Formation. Based on these data, we consider the age of the amber-bearing horizon to be constrained to the Middle–Late Aptian. The age of the amber from this area is comparable to that of the amber from the Damoguaihe Formation in the Zhalainuoer area, eastern Inner Mongolia (Azar *et al*., 2019; Gao *et al*., 2024).

The sporopollen fossil assemblage of the Jiufengshan Formation in the Heibaoshan-Handaqi Basin is broadly comparable to those of the Chengzihe Formation and Muling Formation in the Jixi Basin of Heilongjiang, as well as the Jiufotang Formation and Shahai Formation in western Liaoning (Yang *et al*., 2020). The absolute ages are 125.1–116 Ma for the Chengzihe Formation (Ren *et al*., 2005) and 116–106.9 Ma for the Muling Formation (Yang *et al*., 2005) in the Jixi Basin. The Jiufotang Formation yields an age of approximately 122–115.5 Ma (He *et al*., 2004; Chang *et al*., 2009; Zhang *et al*., 2010). Regional stratigraphic correlation indicates that the Jiufengshan Formation in the Heibaoshan-Handaqi Basin corresponds to the upper-middle part of the Chengzihe Formation and the Jiufotang–Shahai formations, is younger than the Yixian Formation and older than the Muling Formation, and was deposited during the Middle–Late Aptian of the Early Cretaceous.

Material and methods

The Heibaoshan-Handaqi Basin currently contains numerous coal mines. In this study, we collected a total of about 105 amber pieces, as well as some insect and plant fossils, from three coal mines (Jinfeng, Junjin and Zhenxing) in Handaqi Town, Heihe City, Heilongjiang Province (Fig. 1), and one additional collection site with no clear affiliation to a specific coal mine but with the same source as the coal-mine samples.

Amber pieces, insects, and plant fossils were photographed with a Canon EOS 5D Mark II camera equipped with a Canon 100 mm macro lens and coupled to a Zeiss Discovery V16 microscope. Fluorescence photographs were captured using a Canon EOS 5D Mark II camera fitted with a Canon 100 mm macro lens and a 365 nm ultraviolet flashlight.

For Fourier-transform infrared (FT-IR) analysis, amber samples from the Jiufengshan Formation were crushed and homogenised with spectroscopic-grade potassium bromide (KBr). Pellets were prepared using a manual hydraulic press. Spectra were acquired in transmission mode over the wavenumber range of 4000–400 cm^{-1} with a Bruker VERTEX FT-IR spectrophotometer, at a resolution of 4 cm^{-1} and with 40 cumulative scans (Fig. 6).

All described materials are housed in Nanjing Institute of Geology and Palaeontology, CAS, Nanjing, China.

Results

Amber from the Jiufengshan Formation in the Heihe area occurs predominantly in coal seams, with some material occurring in silty mudstone; insects and plants are mainly preserved in yellowish-gray shale. We recovered abundant irregular blocky and layered amber (Figs 2, 3). Only a small number of amber pieces were collected from coal blocks at the Jinfeng Coal Mine, whereas amber is abundant in coal blocks from the Junjin Coal Mine, where a small number of insects were also found in yellowish-gray shale. Amber is densely distributed in coal blocks from the Zhenxing Coal Mine, with some insects and plants discovered in the associated shale. Overall, amber from the Jiufengshan Formation in the Heihe area is widely distributed and abundant in coal seams and is commonly associated with insects and plants, providing important material for studying the palaeoecological environment of this period.

The amber pieces range in size from 0.2 mm to 1.5 cm and occur predominantly as irregular massive and layered forms. Abundant tiny amber fragments are concentrated

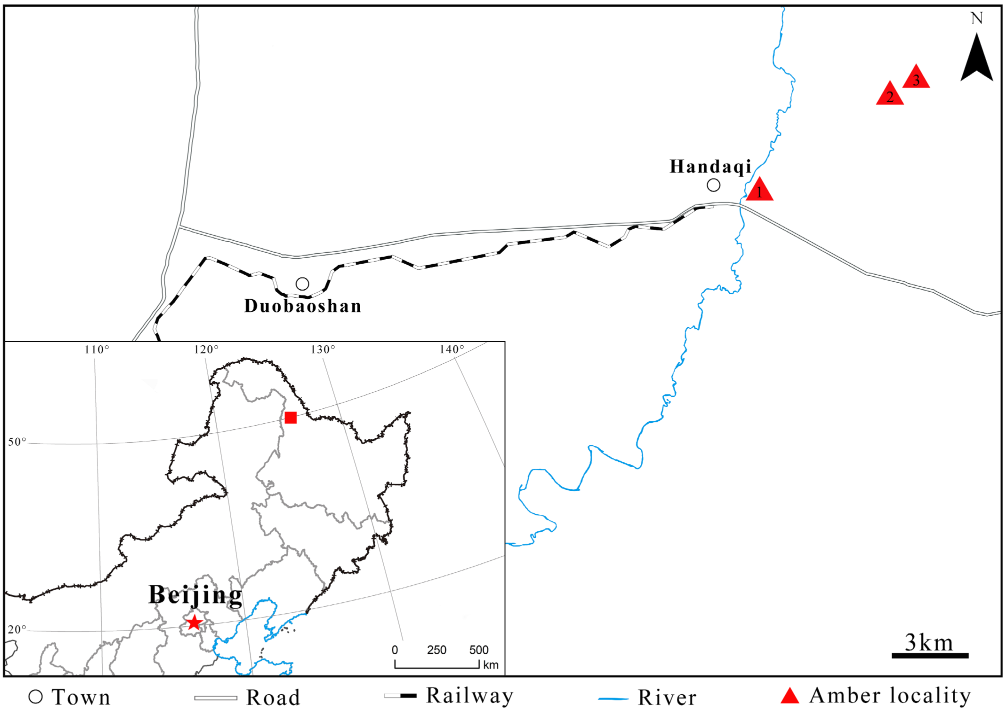

FIGURE 1. Map of the amber locality. Red triangles 1, 2, and 3 mark, respectively, the Jinfeng, Junjin, and Zhenxing coal mines.

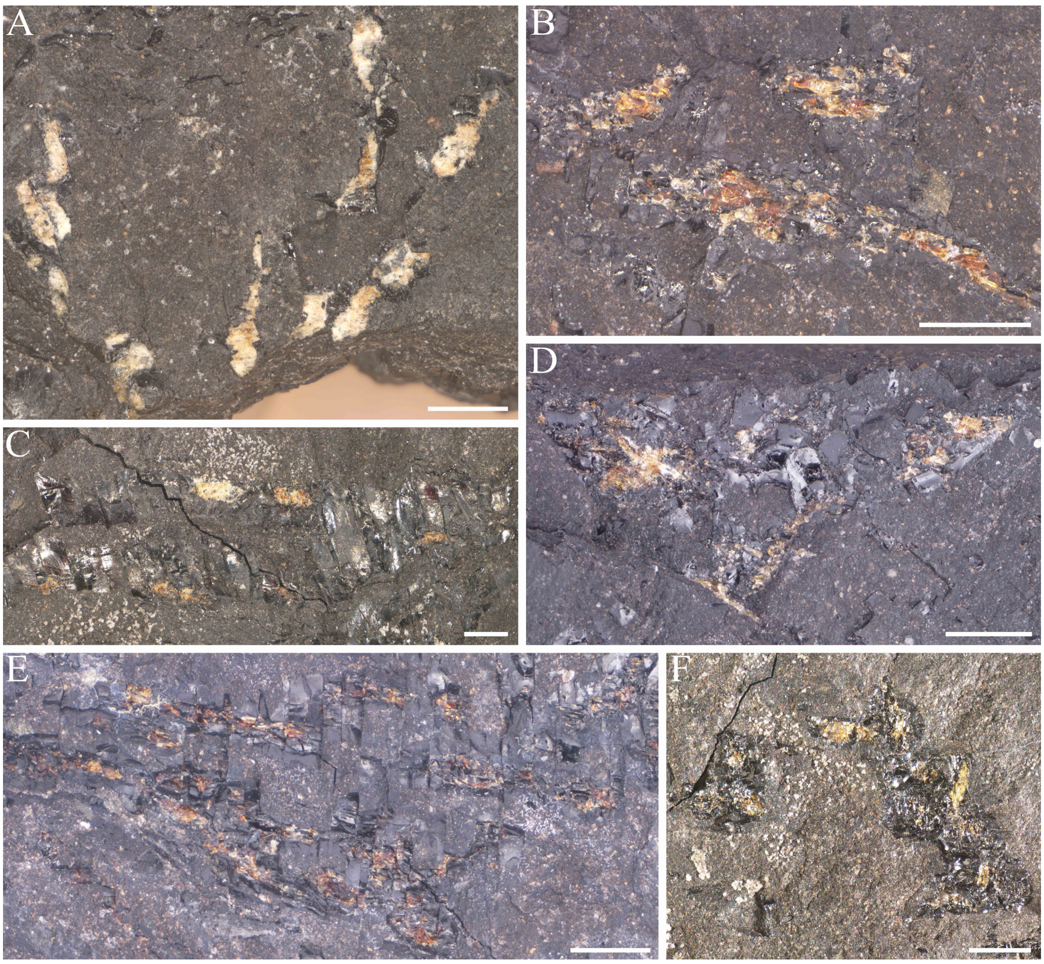

FIGURE 2. Early Cretaceous amber from the Jiufengshan Formation, Handaqi Town, Heilongjiang. **A**, **B**, **D**, **F**, Amber pieces on a bedding surface, NIGP210825(1), 210826(1), 210827, 210829. **C**, **E**, Amber pieces in different layers, NIGP210825(2), 210828(1). Scale bars = 1 mm.

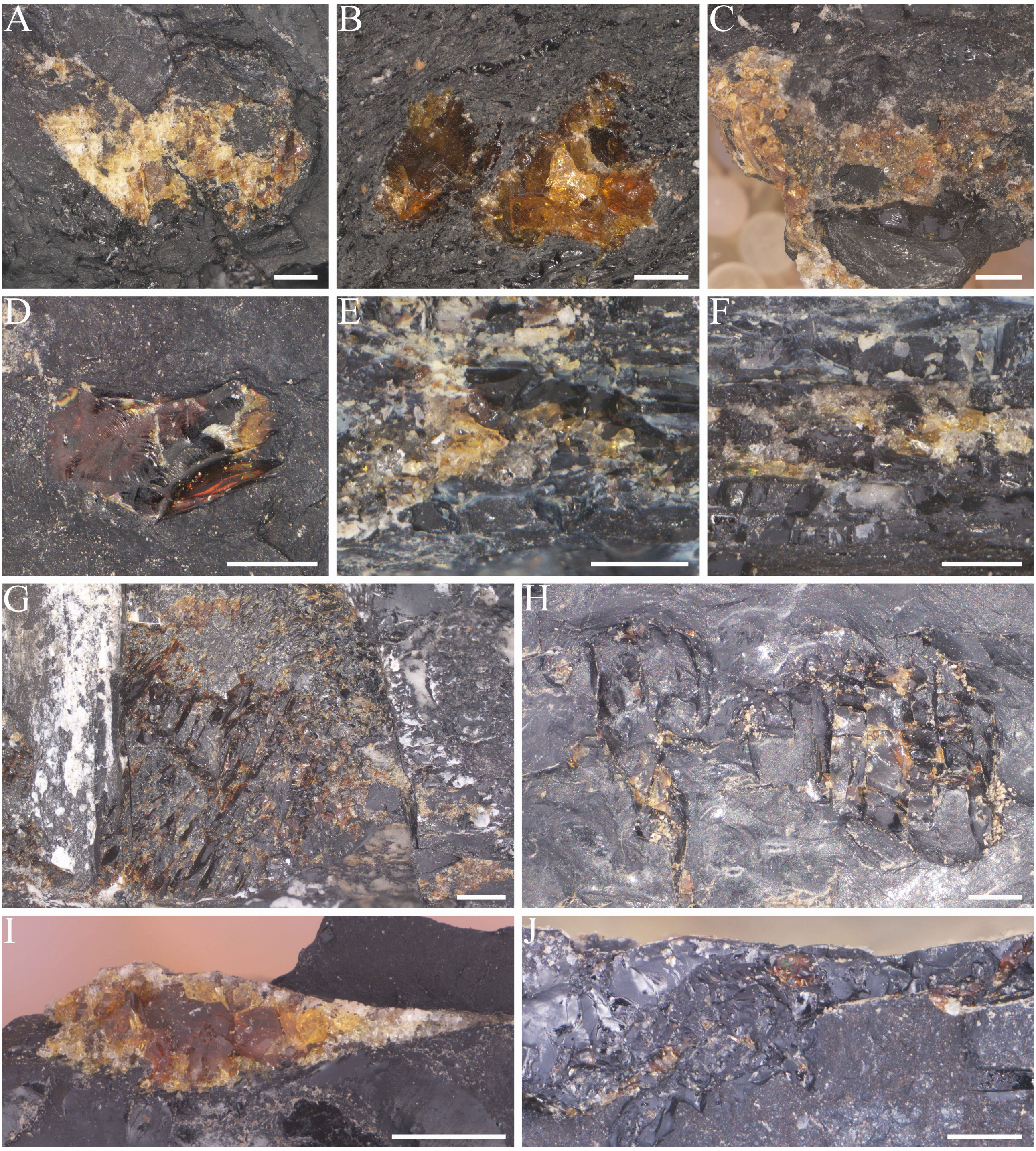

FIGURE 3. Early Cretaceous amber from the Jiufengshan Formation, Handaqi Town, Heilongjiang, of which **A**–**D**, **G**, H are from Junjin, **I** from Jinfeng, and **E**, **F**, **J** from Zhenxing Coal Mine. **A**–**D**, **I**, Irregular amber pieces, NIGP210830–210832, 210833(1), 210836(1). **E**, **F**, Fracture-filling amber, NIGP210834(1), 210834(2). **G**, **H**, Amber pieces in different layers, NIGP210835, 210833(2). **J**, Amber pieces on a bedding surface, NIGP210837. Scale bars = 1 mm for **A**, **B**, **D**, **H**, **I**; 2 mm for **C**, **G**; 500 μm for **E**, **F**, **J**.

in specific horizons of coal blocks (Figs 4G–J; 5C, D, K, L). The amber is mainly transparent, ranging from golden yellow to brownish yellow, and a small number of pieces are opaque yellow. Under ultraviolet light, freshly fractured surfaces of the amber display blue-white fluorescence, while slightly weathered amber shows blue-green fluorescence (Figs 4, 5). No bioinclusions have been found in the amber. These amber pieces often occur as thin layers on coal surfaces or fill fractures within the sediments (Fig. 5G–J), indicating that under the influence of elevated temperatures during coalification, the amber softened, melted into a fluid, and then filled

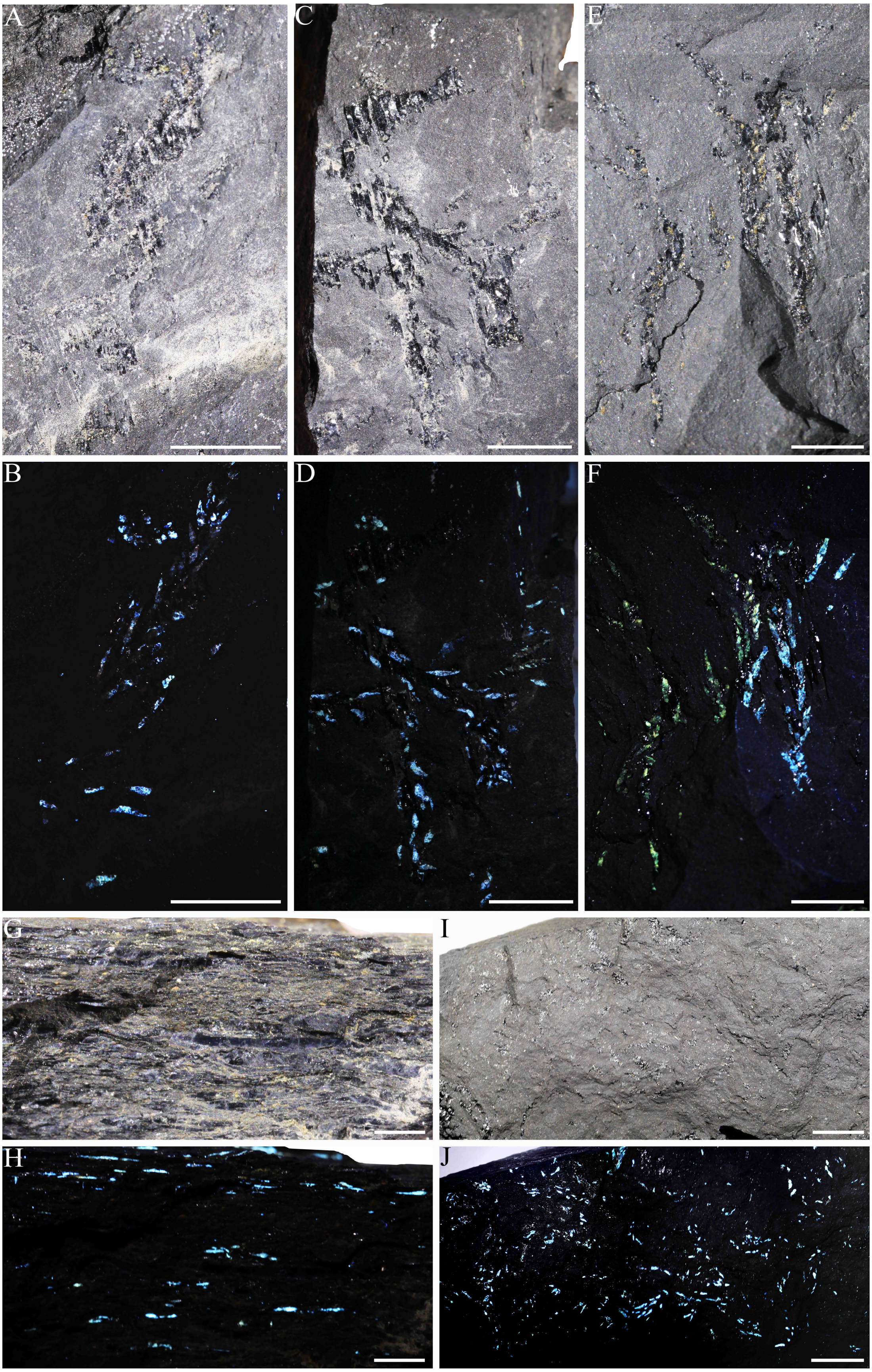

FIGURE 4. Fluorescence of amber from the Lower Cretaceous Jiufengshan Formation, Handaqi Town, Heilongjiang. **A**, **C**, **E**, Amber occurs as intermittent small leaf-like flakes, NIGP210828(2), 210826(2), 210838. **B**, **D**, **F**, Fluorescence photographs of **A**, **C**, and **E**. **G**, Amber pieces in different layers, NIGP210839. **H**, Fluorescence photograph of **G**. **I**, Amber pieces on a bedding surface, NIGP210840. **J**, Fluorescence photograph of **I**. Scale bars = 5 mm for **A**–**F**; 2 mm for **G**, **H**; 1 cm for **I**, **J**.

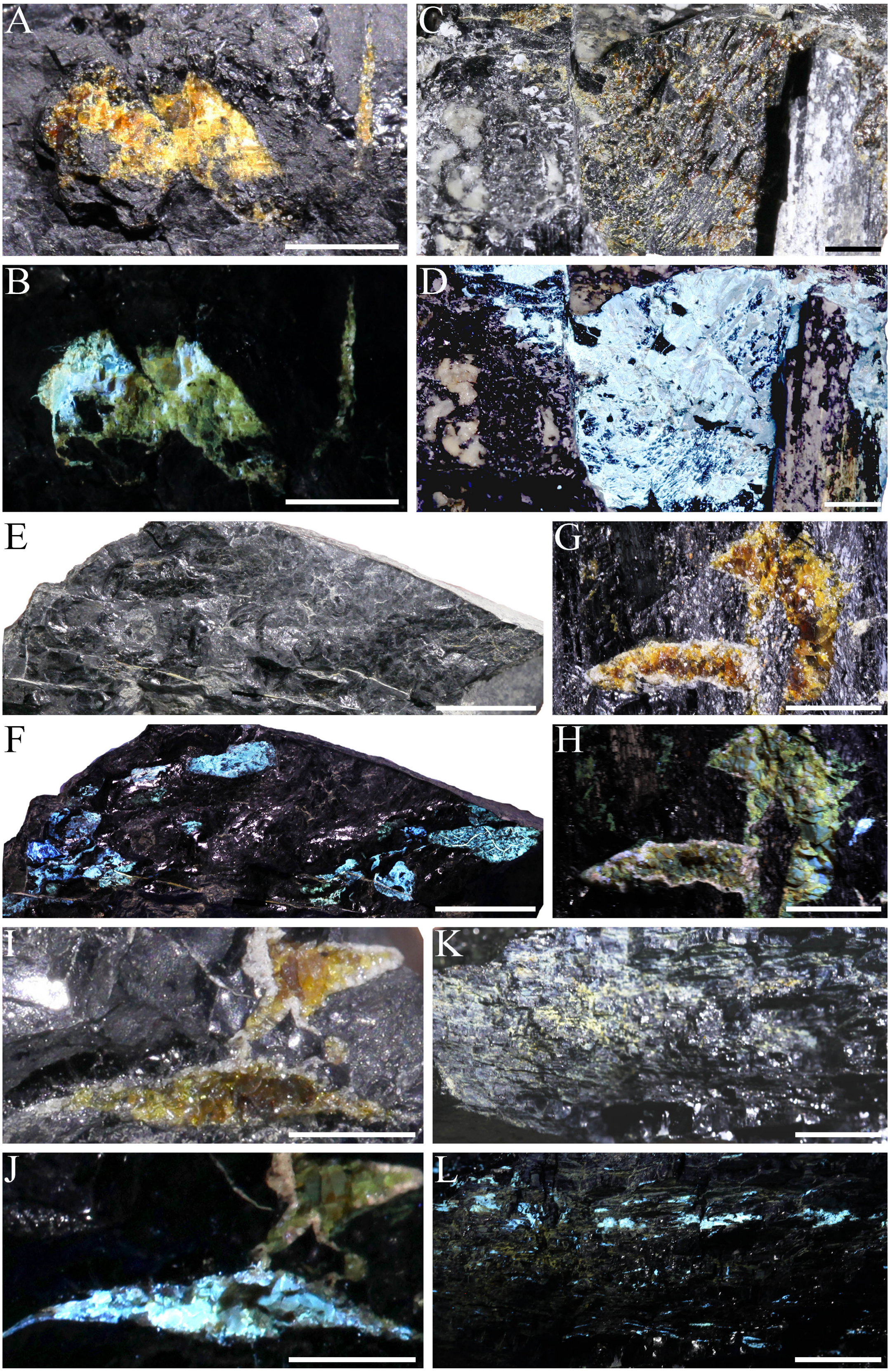

FIGURE 5. Fluorescence of amber from the Lower Cretaceous Jiufengshan Formation, Handaqi Town, Heilongjiang, with **A**–**D**, **G**, **H** from Junjin, **E**, **F**, **K**, **L** from Zhenxing, and **I**, **J** from Jinfeng. **A**, Blocky amber, NIGP210830. **B**, Fluorescence photograph of **A**. **C**, Thin-layered amber, NIGP210835. **D**, Fluorescence photograph of **C**. **E**, Amber pieces on a bedding surface, NIGP210841. **F**, Fluorescence photograph of **E**. **G**, **I**, Fracture-filling amber, NIGP210842, 210836(2). **H**, **J**, Fluorescence photographs of G and I. **K**, Amber pieces in different layers, NIGP210834(3). **L**, Fluorescence photograph of **K**. Scale bars = 3 mm for **A**–**D**; 5 mm for **E**–**H**, **K**, **L**; 2 mm for **I**, **J**.

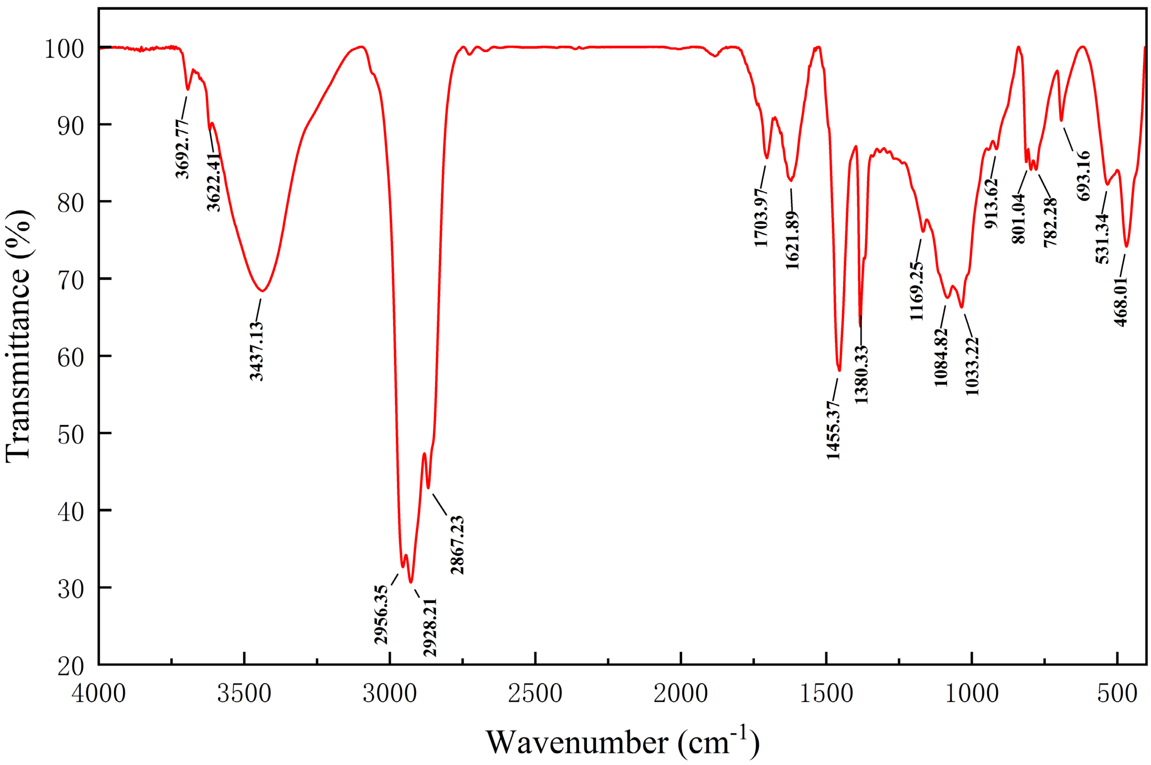

FIGURE 6. FT-IR spectrum of amber samples from the Jiufengshan Formation, Handaqi Town, Heilongjiang.

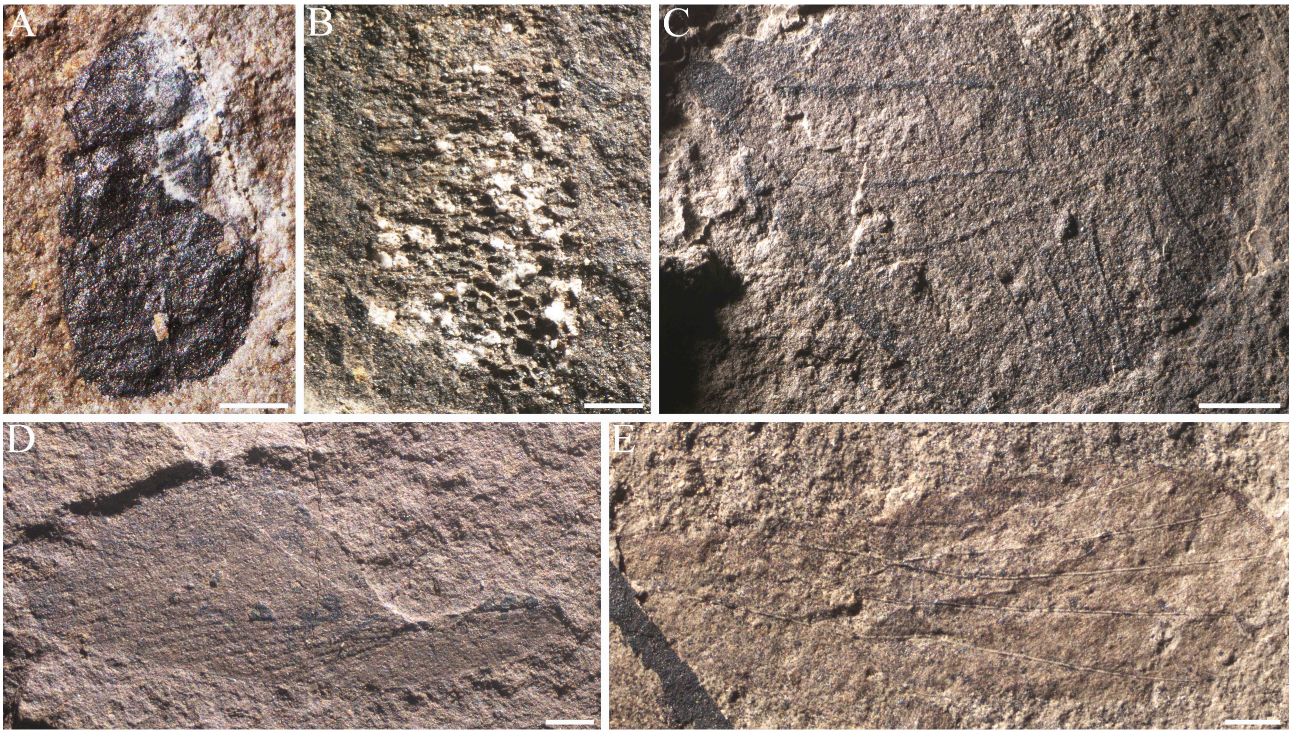

FIGURE 7. Insects from the Lower Cretaceous Jiufengshan Formation, Handaqi Town, Heilongjiang. **A**, Coleoptera, unidentified, NIGP210820. **B**, Caddis case, NIGP210821. **C**, Orthoptera, forewing, unidentified, NIGP210822. **D**, Blattodea, forewing, unidentified, NIGP210823. **E**, Hemiptera, hindwing, unidentified, NIGP210824. Scale bars = 500 μm for **A**, **B**; 1 mm for **C**, **D**, **E**.

interlayer spaces and fractures in the sediments. Many amber pieces appear to have the shape of gymnosperm needle-like leaves, but they are actually exposed portions of thin amber layers broken along lateral edges (Figs 2A, F; 4A–F), and are not biological remains. The margins of these layered amber pieces are commonly transformed into jet, while the centers remain amber, often occurring as intermittent small leaf-like flakes.

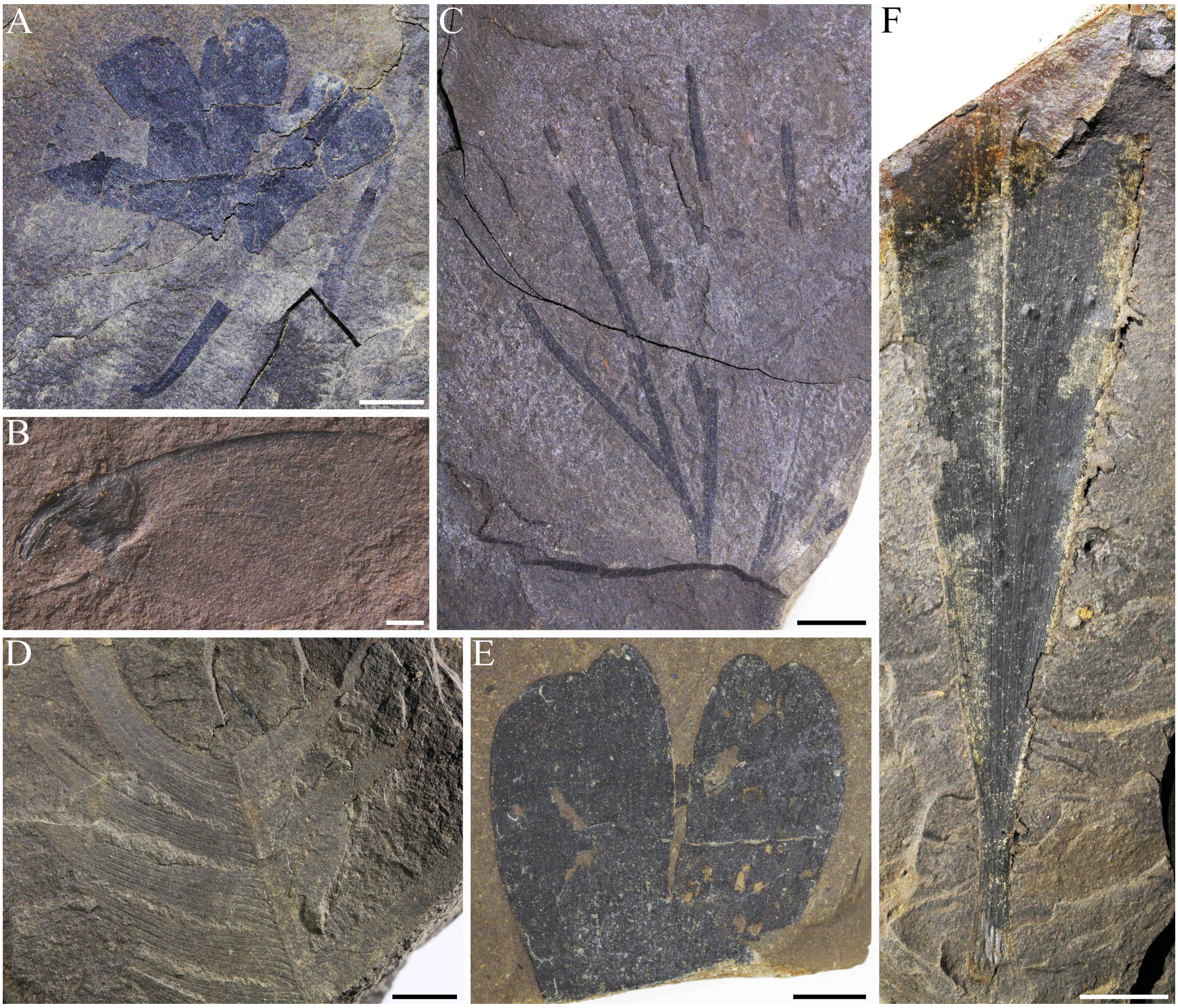

FIGURE 8. Plants from the Lower Cretaceous Jiufengshan Formation, Handaqi Town, Heilongjiang. **A**, *Ginkgoites* sp., NIGP210843. **B**, *Pityospermum* sp., NIGP210844. **C**, *Baiera borealis*, NIGP210845. **D**, *Nilssonia sinensis*, NIGP210846. **E**, *Ginkgoites* sp., NIGP210847. **F**, *Sphenobaiera* sp., NIGP210848. Scale bars = 5 mm for **A**, **C**, **D**, **E**; 1 mm for **B**; 10 mm for **F**.

The shale yields diverse insects, including Coleoptera, Orthoptera, Hemiptera, Blattodea, and caddis cases (Fig. 7). Plants include *Ginkgoites* sp., *Pityospermum* sp., *Baiera borealis*, *Nilssonia sinensis* and *Sphenobaiera* sp. (Fig. 8). The insect and plant fossils discovered so far are few in number and moderately preserved, and have not yet been studied in detail.

Fourier-transform infrared (FT-IR) analysis was performed on the Heihe amber to characterize its chemical features and compare its structural characteristics with those of known amber types. Although FT-IR alone is insufficient to accurately determine botanical origin because many ambers have broadly similar spectra (Azar *et al.*, 2010), it effectively identifies key functional groups and distinguishes major fossil-resin classes. The sharp absorption peaks at 3693 cm^{-1} and 3622 cm^{-1} correspond to the stretching vibrations of free alcoholic hydroxyl (-OH) groups, while the strong and broad absorption band at 3437 cm^{-1} is assigned to the stretching vibration of hydrogen-bonded O-H, with both signal types originating from alcoholic hydroxyl groups or trace adsorbed moisture in the resin. The absorption peaks at 2956 cm^{-1}, 2928 cm^{-1}, and 2867 cm^{-1} are attributed to aliphatic C-H stretching vibrations, which are characteristic signals of CH, CH_2, and CH_3 groups in the terpenoid skeleton of the resin. The distinct transmittance peak at 1704 cm^{-1} corresponds to the C=O stretching vibration of conjugated carbonyl groups. The absorption peak at 1622 cm^{-1} is assigned to the C=C stretching vibration of alkenyl groups. The transmittance peaks at 1455 cm^{-1} and 1380 cm^{-1} correspond to CH_2/CH_3 bending vibrations, and are typical of aliphatic chains; of these, the absorption peak at 1380 cm^{-1} specifically represents the CH_3 symmetric deformation vibration, a common characteristic of fossil resins. The absorption peaks at 1169 cm^{-1}, 1084 cm^{-1}, and 1033 cm^{-1} are attributed to the C-O stretching vibration of ether or ester linkages, which is consistent with the characteristics of oxygen-containing functional groups in polymerized resin structures. The characteristic absorption at 913 cm^{-1} in the low-wavenumber region corresponds to the out-of-plane C-H bending vibration of terminal exomethylene (=CH_2) groups. This diagnostic peak is characteristic of labdanoid diterpenes (Class I amber). Its presence strongly supports a possible coniferous botanical origin.

In summary, the FT-IR spectrum confirms that the Heihe amber studied herein contains the typical aliphatic and oxygenated functional groups of polymerized diterpenoid resin. Moreover, the observed peaks are consistent with typical spectra of fossilized resins, particularly those of Class I (polylabdanoid) ambers. However, FT-IR alone does not provide sufficient resolution to determine exact botanical provenance with high accuracy. Therefore, the results should be interpreted cautiously.

Conclusion

Integrating these results with regional palaeobotanical and palynological data, the flora of the Jiufengshan Formation in the Heibaoshan-Handaqi Basin is dominated by gymnospermous conifers, and its sporopollen assemblage is also dominated by gymnosperm pollen, with no angiosperm fossils or pollen recovered. Thus, the amber in this area probably originated from gymnosperms.

The discovery of amber, insects, and plants from the Jiufengshan Formation in the Heibaoshan-Handaqi Basin enriches the Late Mesozoic palaeobiodiversity of the Jiufengshan Formation and the Heihe area. These findings provide important evidence for reconstructing the palaeovegetation of the Jiufengshan Formation, and also provide new data for studies of Mesozoic amber in China.

Acknowledgements

The authors are grateful to two anonymous reviewers for their helpful comments on the manuscript. Financial support was provided by the National Key Research and Development Program of China (2024YFF0807601) and the National Natural Science Foundation of China (42430211, 42288201).

References

Azar, D., Gèze, R. & Acra, F. (2010) Chapter 14: Lebanese amber. *In*: Penney, D. (Ed.), *Biodiversity of fossils in amber from the major world deposits*. Siri Scientific Press, Manchester, pp. 271–298.

Azar, D., Maksoud, S., Cai, C.Y. & Huang, D.Y. (2019) A new amber outcrop from the Lower Cretaceous of northeastern China. *Palaeoentomology*, 2 (4), 345–349. https://doi.org/10.11646/palaeoentomology.2.4.8

Bouju, V. & Perrichot, V. (2020) A review of amber and copal occurrences in Africa and their paleontological significance. *BSGF—Earth Sciences Bulletin*, 191 (17), 1–11. https://doi.org/10.1051/bsgf/2020018

Bugdaeva, E.V., Nosova, N.V., Sun, G., Liang, F., Golovneva, L.B. & Song, Y. (2025) The Coal-Forming plants of Early Cretaceous resin coals of the southern Primorye (Russia) and Heilongjiang Province (China). *Russian Journal of Pacific Geology*, 19 (6), 671–682. https://doi.org/10.1134/S1819714025700460

Bureau of Geology and Mineral Resources of Heilongjiang Province. (1993) *Regional Geology of Heilongjiang Province*. Geology Press, Beijing, 734 pp. [In Chinese]

Bureau of Geology and Mineral Resources of Heilongjiang Province. (1997) *Lithostratigraphy of Heilongjiang Province*. China University of Geosciences Press, Wuhan, 298 pp. [In Chinese]

Chang, S.C., Zhang, H.C., Renne, P.R. & Fang, Y. (2009) High-precision $^{40}Ar/^{39}Ar$ age for the Jehol biota. *Palaeogeography, Palaeoclimatology, Palaeoecology*, 280, 94–104. https://doi.org/10.1016/j.palaeo.2009.06.021

Delclòs, X., Arillo, A., Peñalver, E., Barrón, E., Soriano, C., López Del Valle, R., Bernárdez, E., Corral, C. & Ortuño, V.M. (2007) Fossiliferous amber deposits from the Cretaceous (Albian) of Spain. *Comptes Rendus Palevol*, 6 (1–2), 135–149. https://doi.org/10.1016/j.crpv.2006.09.003

Delclòs, X., Peñalver, E., Barrón, E., Peris, D., Grimaldi, D.A., Holz, M., Labandeira, C.C., Saupe, E.E., Scotese, C.R., Solórzano-Kraemer, M.M., Álvarez-Parra, S., Arillo, A., Azar, D., Cadena, E.A., Dal Corso, J., Kvaček, J., Monleón-Getino, A., Nel, A., Peyrot, D., Bueno-Cebollada, C.A., Gallardo, A., González-Fernández, B., Goula, M., Jaramillo, C., Kania-Kłosok, I., López-Del Valle, R., Lozano, R.P., Meléndez, N., Menor-Salván, C., Peña-Kairath, C., Perrichot, V., Rodrigo, A., Sánchez-García, A., Santer, M., Sarto i Monteys, V., Uhl, D., Viejo, J.L. & Pérez-de la Fuente, R. (2023) Amber and the Cretaceous resinous interval. *Earth-Science Reviews*, 243, 104486. https://doi.org/10.1016/j.earscirev.2023.104486

Gao, H.L., Su, Y.T., Cai, C.Y., Azar, D., Song, X.B., Lian, X.N. & Huang, D.Y. (2024) Discussion on the age of the Early Cretaceous amber from the Hailar Basin, NE China. *Mesozoic*, 1 (2), 192–207. https://doi.org/10.11646/mesozoic.1.2.11

Grimaldi, D., Beck, C.W. & Boon, J.J. (1989) Occurrence, chemical characteristics, and paleontology of the fossil resins from New Jersey. *American Museum Novitates*, 2948, 1–28.

Grimaldi, D.A., Engel, M.S. & Nascimbene, P.C. (2002) Fossiliferous Cretaceous amber from Myanmar (Burma): its rediscovery, biotic diversity, and paleontological significance. *American Museum Novitates*, 3361, 1–71. https://doi.org/10.1206/0003-0082(2002)361<0001:FCAFMB>2.0.CO;2

Guo, X. (2024) *Paleoenvironmental Significance of Biomarkers in Early Cretaceous Coals in Huola Basin*. Hebei University of Engineering, Handan, 77 pp. [In Chinese] https://doi.org/10.27104/d.cnki.ghbjy.2024.000041

Han, Z.Z., Li, Z.D., Sun, G.R. & Yin, Z.G. (2000) The first finds of the Mesozoic fish fossil (*Genus Asiatorepis* Takai) in the west of Heilongjiang Province and its geological significance. *Heilongjiang Geology*, 11 (3), 8–14. [In Chinese]

He, H.Y., Wang, X.L., Zhou, Z.H., Wang, F., Boven, A., Shi, G.H. & Zhu, R.X. (2004) Timing of the Jiufotang Formation (Jehol Group) in Liaoning, northeastern China, and its implications. *Geophysical Research Letters*, 31 (12), L12605. https://doi.org/10.1029/2004GL019790

Huber, B.T., Norris, R.D. & MacLeod, K.G. (2002) Deep-sea paleotemperature record of extreme warmth during the Cretaceous. *Geology*, 30 (2), 123–126. https://doi.org/10.1130/0091-7613(2002)030<0123:DSPROE>2.0.CO;2

Ji, G.Z., Cai, C.Y., Yu, X.F., Azar, D., Dong, C., Song, X.B., Wang, Y.H., Xu, M.M. & Huang, D.Y. (2025) Distribution and mineralogical characteristics of amber in the Upper Cretaceous Gaogou Formation in Xixia, Henan Province, China. *Mesozoic*, 2 (1), 60–69. https://doi.org/10.11646/mesozoic.2.1.8

Jia, X.H., Liang, C.Y. & Zheng, C.Q. (2025) Detrital zircon U–Pb ages of sandstone from Jiufengshan Formation in Nenjiang area, Heilongjiang Province: Provenance and tectonic implications. *Global Geology*, 28 (2), 79–98. https://doi.org/10.3969/j.issn.1673-9736.2025.02.01

Jin, R.S. (1997) Discovery of the plant fossil and significance of the ascertained age in the Jiufengshan Formation, the Oupu Basin, Huma County. *Heilongjiang Geology*, 8 (2), 6–17. [In Chinese]

Klages, J.P., Gerschel, H., Salzmann, U., Nehrke, G., Müller, J., Hillenbrand, C.D., Bohaty, S.M. & Bickert, T. (2024) First discovery of Antarctic amber. *Antarctic Science*, 36 (5), 439–440. https://doi.org/10.1017/S0954102024000208

Kubota, A., Takeda, Y., Yi, K., Sano, S. & Iba, Y. (2025) Amber in the Cretaceous deep sea deposits reveals large-scale tsunamis. *Scientific Reports*, 15, 14298. https://doi.org/10.1038/s41598-025-96498-2

Langenheim, R.L., Jr., Smiley, C.J. & Gray, J. (1960) Cretaceous amber from the Arctic coastal plain of Alaska. *Bulletin of the Geological Society of America*, 71 (9), 1345–1356. https://doi.org/10.1130/0016-7606(1960)71[1345:CAFTAC]2.0.CO;2

Li, X.B. & Reisz, R. (2020) The stratigraphy and paleoenvironment of a '*Lycoptera* Bed' site in eastern Inner Mongolia, China: correlation with the fossiliferous Lower Cretaceous strata in western Liaoning. *Palaeogeography, Palaeoclimatology, Palaeoecology*, 559, 109951. https://doi.org/10.1016/j.palaeo.2020.109951

Li, Y.L., Zheng, D.R., Li, X.B., Teng, X., Zhang, Q.Q., Wang, H., Lee, H.Y., Wang, B. & Chang, S.C. (2023a) New age constraints on the Lower Cretaceous Jiufengshan Formation of Inner Mongolia, China and their implications for the spatiotemporal development of the Jehol biota. *Palaeogeography, Palaeoclimatology, Palaeoecology*, 629, 111787. https://doi.org/10.1016/j.palaeo.2023.111787

Li, Y.L., Zheng, D.R., Sha, J.G., Zhang, H.C., Denyszyn, S. & Chang, S.C. (2023b) Lower Cretaceous Hailar amber: The oldest-known amber from China. *Cretaceous Research*, 145, 105472. https://doi.org/10.1016/j.cretres.2022.105472

Luo, L.H. & Huang, D.Y. (2026) Late Cretaceous amber from Jiayin (Heilongjiang Province, northeastern China) and wildfire events. *Palaeoentomology*, 9 (2), 189–199. https://doi.org/10.11646/palaeoentomology.9.2.11

Maksoud, S., Granier, B.R.C. & Azar, D. (2022) Palaeoentomological (fossil insects) outcrops in Lebanon. *Carnets de Géologie*, 22 (16), 699–743. https://doi.org/10.2110/carnets.2022.2216

McKellar, R.C., Wolfe, A.P., Tappert, R. & Muehlenbachs, K. (2008) Correlation of Grassy lake and Cedar lake ambers using infrared spectroscopy, stable isotopes, and palaeoentomology. *Canadian Journal of Earth Sciences*, 45 (9), 1061–1082. https://doi.org/10.1139/E08-049

Najarro, M., Peñalver, E., Pérez-De La Fuente, R., Ortega-Blanco, J., Menor-Salván, C., Barrón, E., Soriano, C., Rosales, I., López Del Valle, R., Velasco, F., Tornos, F., Daviero-Gomez, V., Gomez, B. & Delclòs, X. (2010) Review of the El Soplao amber outcrop, Early Cretaceous of Cantabria, Spain. *Acta Geologica Sinica* (*English Edition*), 84 (4), 959–976. https://doi.org/10.1111/j.1755-6724.2010.00258.x

Néraudeau, D., Perrichot, V., Colin, J.P., Girard, V., Gomez, B., Guillocheau, F., Masure, E., Peyrot, D., Tostain, F., Videt, B. & Vullo, R. (2008) A new amber deposit from the Cretaceous (uppermost Albian–lowermost Cenomanian) of southwestern France. *Cretaceous Research*, 29 (5-6), 925–929. https://doi.org/10.1016/j.cretres.2008.05.009

Ni, Z.J., Song, X.B., Azar, D., Wang, Z.X., Cai, C.Y., Xuan, Q., Maksoud, S., Lian, X.N. & Huang, D.Y. (2023) Discovery of Late Cretaceous amber from Guangzhou, South China. *Palaeoentomology*, 6 (4), 329–332. https://doi.org/10.11646/palaeoentomology.6.4.3

Perkovsky, E.E. & Vasilenko, D.V. (2019) A summary of recent results in the study of Taimyr amber. *Paleontological Journal*, 53 (10), 984–993. https://doi.org/10.1134/S0031030119100149

Ren, F.H., Yang, X.P., Li, Y.C., Wang, Y. & Zhou, X.F. (2005) Chronostratigraphic division of the Jixi Group in eastern Heilongjiang Province and its geological significance. *Geology in China*, 32 (1), 48–54. [In Chinese]

Ross, A.J. (2024) Complete checklist of Burmese (Myanmar) amber taxa 2023. *Mesozoic*, 1 (1), 21–57. https://doi.org/10.11646/mesozoic.1.1.4

Shi, G.L., Dutta, S., Paul, S., Wang, B. & Jacques, F.M.B. (2014) Terpenoid compositions and botanical origins of Late Cretaceous and Miocene amber from China. *PLoS One*, 9 (10), e111303. https://doi.org/10.1371/journal.pone.0111303

Song, X.B., Sui, X., Xuan, Q., Azar, D., Cai, C.Y., Wang, Z.X. & Huang, D.Y. (2024) A new amber outcrop from the Late Cretaceous of Xingning Basin, South China. *Palaeoentomology*, 7 (6), 770–777. https://doi.org/10.11646/palaeoentomology.7.6.12

Tihelka, E., Jarzembowski, E.A., Azar, D., Huang, D.Y. & Cai, C.Y. (2023) An unusual artematopodid beetle from Early Cretaceous Wealden amber (Coleoptera: Elateroidea: Artematopodidae). *Palaeoentomology*, 6 (5), 445–458. https://doi.org/10.11646/palaeoentomology.6.5.4

Yang, X.P., Ma, Y.Q., Hao, Y.H., Wang, H.J. & Li, Y.C. (2005) Chronostratigraphic classification of Muling Formation, Jixi Group in eastern Heilongjiang Province. *Geology and Resources*, 14 (3), 166–169. [In Chinese] https://doi.org/10.13686/j.cnki.dzyzy.2005.03.002

Yang, Y.J., Jiang, B., Wang, X.Z., Pang, X.J. & Shi, G.M. (2020) Chronostratigraphic division of the Early Cretaceous Jiufengshan Formation in Heibaoshan–Handaqi Basin, Heilongjiang Province. *Geology and Resources*, 29 (5), 403–410. [In Chinese] https://doi.org/10.13686/j.cnki.dzyzy.2020.05.001

Zhang, H.C., Wang, B. & Fang, Y. (2010) Evolution of insect diversity in the Jehol biota. *Scientia Sinica* (*Terrae*), 40 (9), 1266–1276. [In Chinese] https://doi.org/10.1007/s11430-010-4098-5

Zhang, Y., Barreiro, I.R., Wan, C.B., Ge, W.C., Wang, G.C., Xue, Y.F., Li, T. & Zhang, X. (2026) Integrative palynology and U–Pb zircon geochronology of the Jiufengshan Formation (upper Aptian, Dayangshu Basin, NE China): evidence for early angiosperm expansion at mid-latitudes. *Palaeogeography, Palaeoclimatology, Palaeoecology*, 691, 113728. https://doi.org/10.1016/j.palaeo.2026.113728

Zhao, F.M., Lu, M.Q., Yan, Y.J., Liu, X.M., Wang, X.C. & Wu, D. (1991) The sedimentary structure and the characteristics of accumulation in the Late Jurassic in the Heibaoshan–Mu'erqi Basin. *Journal of Changchun University of Earth Science*, 21 (4), 411–416. [In Chinese]